Low-Loss Ku-Band Artificial Transmission Line With MEMS Tuning Capability

Julien Perruisseau-Carrier, *Member, IEEE*, Kagan Topalli, *Member, IEEE*, and Tayfun Akin, *Member, IEEE*

***Abstract*—An artificial transmission line unit cell is presented based on the so-called composite right/left handed transmission line. It is implemented on a microelectromechanical system process on glass, and is suitable for applications such as reconfigurable leaky-wave antennas and series feed networks. The device presents state-of-the-art performance in terms of differential phase shift over losses ($38^\circ/\mathrm{dB}$ at 14 GHz) and quasi-zero drive power consumption. It is monolithic and has a total footprint of 4 mm^2.**

***Index Terms*—Artificial transmission line, composite right/left-handed (CRLH), metamaterial, microelectromechanical system (MEMS), reconfigurable.**

I. Introduction

A wide range of microwave devices with enhanced performances have been developed using the particular dispersion of the composite right/left handed transmission line (CRLH-TL) structure [1], [2]. However, although high frequency operation and tuning capabilities are strongly desirable in modern microwave systems, the devices initially designed were non-reconfigurable and operated at rather low frequencies (<6 GHz). In this context, several groups have recently studied the implementation of higher frequency micromachined (e.g. [3], [4]) and reconfigurable (e.g. [5]–[9]) CRLH structures.

Microelectromechanical system (MEMS) technology is an excellent candidate to simultaneously meet the challenges of high frequency operation and reconfigurability, while preserving low insertion loss, high linearity, and quasi-zero drive power consumption. In this letter, we present a reconfigurable CRLH unit cell based on a coplanar waveguide (CPW) and monolithically integrated on a MEMS process. The cell is designed to exhibit a controllable frequency of 0° phase shift in Ku band.

Section II describes the proposed CRLH unit cell and its MEMS structure. Measured results under actuation are presented in Section III, showing good agreement with full-wave simulations. Finally, Section IV discusses the performances of the device, in comparison to previous works and in the light of potential applications, demonstrating state-of-the-art performance in terms of differential phase shift over losses, high operation frequency, and compactness.

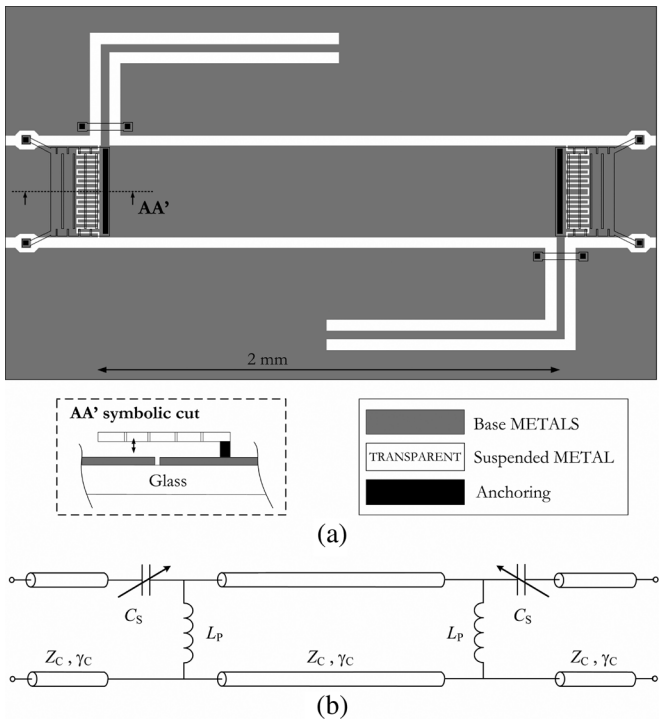

Fig. 1. (a) Layout of the CRLH unit cell and cross-sectional view of the MEMS capacitor. For clarity, the two first metal layers are shown as one (base metals) and dielectric and sacrificial layers are omitted. (b) Corresponding CRLH unit cell circuit model (without parasitic elements).

II. Description

The device layout and its associated conceptual circuit model are shown in Fig. 1, and Fig. 2 presents the measured profile of the MEMS area of the fabricated circuit. The cell consists of a CPW loaded by folded shunt stub inductors and series MEMS capacitors. It was fabricated using an in-house MEMS process developed at METU on 500 μm-thick glass wafers ($\varepsilon_r = 4.6$, $\tan\delta = 0.01$) presented in [10].

As can be seen in the cross section inset of Fig. 1 and in the profile of Fig. 2, the series capacitance consists of the combination of a fixed interdigited capacitor and a movable MEMS membrane, to provide sufficient degrees of freedom in the electromagnetic-electromechanical design. The membrane is anchored at one of its extremity as a cantilever. In order to control the effect of residual stress on the membrane shape, slots have been etched perpendicular to the membrane, and two

Manuscript received February 03, 2009; revised February 18, 2009. First published May 26, 2009; current version published June 05, 2009. This work was supported by the Spanish government Torres Quevedo Grant PTQ-08-01-06434 and the European Union COST Action IC0603.

J. Perruisseau-Carrier is with the Centre Tecnologic de Telecomunicacions de Catalunya (CTTC), Barcelona, Spain (e-mail: julien.perruisseau@cttc.es).

K. Topalli and T. Akin are with Department of Electrical and Electronics Engineering, Middle East Technical University, Ankara 06531, Turkey.

Color versions of one or more of the figures in this letter are available online at http://ieeexplore.ieee.org.

Digital Object Identifier 10.1109/LMWC.2009.2020022

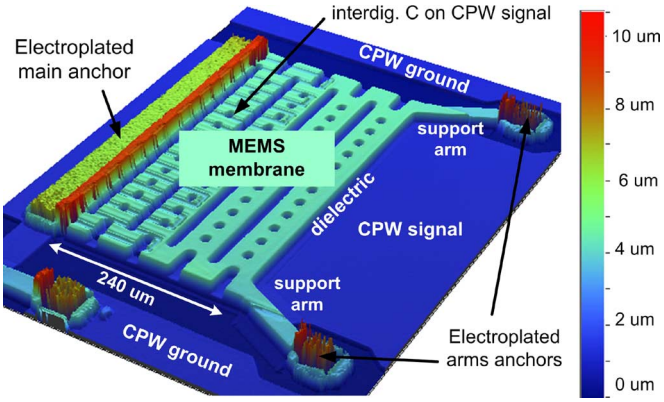

Fig. 2. Measured profile of the non-actuated fabricated MEMS. The membrane is suspended over the targeted air gap of 2 μm and exhibits good planarity.

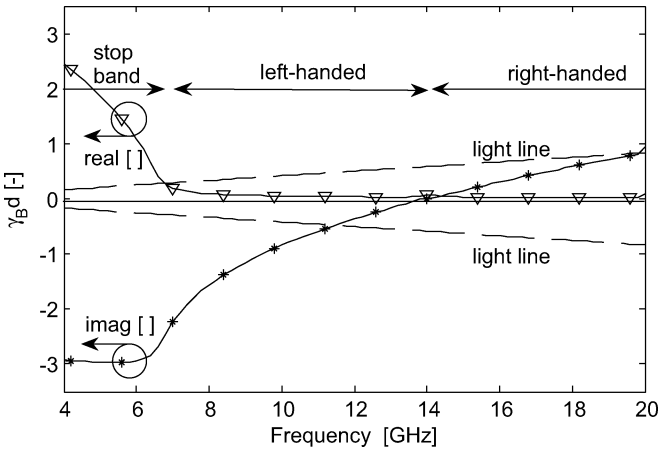

Fig. 3. Simulated Bloch–Floquet propagation constant of the MEMS CRLH unit cell without actuation (using Ansoft HFSS).

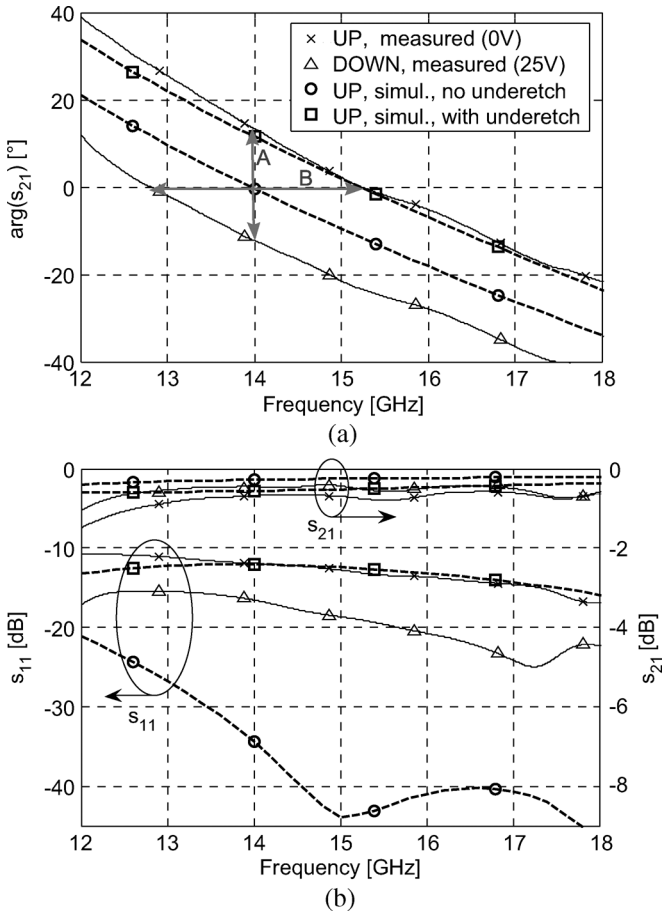

Fig. 4. Measured and simulated S-parameters of the MEMS CRLH unit cell.

small "support arms" have been added on the MEMS non-anchored corners. As can be seen in Fig. 2, this leads to good membrane planarity, with a maximum measured deflection within the whole membrane inferior to 2000 Å (significant bowings have been observed in similar structures without slots or additional anchor arms).

The bottom electrode of the MEMS is part of the central conductor of the CPW in the middle of the cell, which is dc-grounded by the inductive stubs. Concerning the movable membrane, it is connected by the main anchor to the CPW central conductor at the cell input/output. Therefore, the MEMS structure can be actuated by applying a voltage between CPW signal line and grounds at the cell input/output (for instance by means of the measurement RF probes). In the case where several cells must be cascaded, the desired actuation can be obtained by the use of dc-block capacitors and high resistivity bias lines (available in the process [10]).

III. Simulations and Measurements

The simulated Bloch–Floquet propagation constant γ_B of the non-actuated device is shown in Fig. 3, where d is the length of the unit cell (2 mm). A typical CRLH-TL dispersion is obtained [1], [2], and the different bands are highlighted in the graph. The frequency of 0° phase shift, corresponding to the transition between left and right-handed bands, is $f_0 = 14$ GHz.

The MEMS membrane is actuated by a bipolar waveform of period of 1 kHz having rise and fall times of less than 100 ns, which is much smaller than the membrane mechanical response. Thus, the bipolar waveform acts as a DC actuation voltage, while minimizing charging effects to avoid drift in the actuation voltage. The measured actuation voltage of the MEMS membrane is 18 V, but a better contact is achieved by increasing the voltage up to 25 V.

The measurements were carried out on-wafer using a thru-reflect-line (TRL) calibration, and S-parameters results at 0 V and 25 V are shown in Fig. 4. Simulation results for the non-actuated MEMS are plotted for comparison with the measurements. We show the results corresponding to the targeted device dimensions (i.e. corresponding to the Bloch-Floquet propagation constant of Fig. 3), but also taking into account in the simulations the measured underetching of 6 μm of the base metal in the fabricated device.

First, it is observed that a good agreement is obtained between measurements and simulations including the measured underetching $\times$ and $\square$ markers), hence validating simulation results. Second, the comparison between simulations with and without underetching $\circ$ and $\square$ markers) reveals that the underetching leads to some deviation in f_0 (which is now about 15.2 GHz),

and a degradation of the matching, which nevertheless remains better than -12 dB in the whole Ku band.

IV. Performance and Applications

In order to discuss the performance of the presented device, we differentiate two applications for controllable CRLH cells. The first one concerns leaky wave antennas scanning around broadside [1], [2], [7]. This application relies on the ability of the CRLH cell to exhibit a controllable negative/zero/positive phase shift at a given frequency, as symbolized by the arrow "A" in Fig. 4. The presented MEMS-based cell exhibits a measured phase shift reconfigurable from $-13°$ to $+13°$ at 14 GHz with maximum insertion loss of 0.68 dB. This corresponds to a differential phase shift over losses figure of merit (FoM) of $38°/\mathrm{dB}$ at 14 GHz. It is worth mentioning that a better figure would have been obtained without underetching in the fabricated structure. Indeed, the FoM is limited by the insertion loss of 0.68 dB measured at 0 V. As explained in Section III, the underetching results in a higher mismatch in this state, which also leads to degradation of the magnitude of S_{21} from -0.3 dB to -0.6 dB in the simulations.

Nevertheless, a survey of reconfigurable CRLH unit cells reveals that the measured FoM of $38°/\mathrm{dB}$ is the highest obtained above 6.5 GHz. Indeed, there are only two CRLH unit cells exhibiting superior FoM, which operate at lower frequencies than 14 GHz. The first one uses varactor diodes and exhibits $60°/\mathrm{dB}$ at 6.5 GHz [5]. The second device is one of the devices presented in [7], which is based on a MMIC mounted on printed elements and achieves $128°/\mathrm{dB}$ at 2.5 GHz. In addition to its higher operation frequency, the device presented in this work is fully monolithic and more compact ($4\ \mathrm{mm}^2$). It also presents the advantages inherent to MEMS technology, namely, high linearity and quasi-zero drive power consumption. Finally, it is worth mentioning that monolithic cells have also been presented based on various technologies [6]–[9], but they all present lower FoM (the FoM for most of these devices are reported in [6, Fig.6]).

The second main application concerns CRLH-based series feed networks or dividers [1], [2]. Such devices operate at the frequency of 0° phase shift f_0 of the CRLH unit cell. Thus, their operation frequency could be dynamically controlled by varying f_0, as shown here by the arrow 'B' in Fig. 4. In this case, the performance of the device should rather be expressed in terms of the relative tunability of f_0 and the maximum corresponding losses, which are here 18% and 0.8 dB, respectively. The advantages of the proposed cell with respect to this second application are similar to the case of the leaky-wave antenna detailed above.

Finally, it is worth mentioning that some distributed MEMS transmission lines (DMTL) exhibit better differential phase shift over losses FoM than all reconfigurable CRLH cells (e.g. $170°/\mathrm{dB}$ [11]). However, the DMTL exhibits a true-time differential delay, and is thus not suitable for the leaky-wave antenna and series feed network applications, which rely on the particular dispersion of the CRLH structure.

V. Conclusion

We have presented a monolithic MEMS implementation of an artificial transmission line CRLH unit cell. It provides simultaneously high frequency operation, low loss and compactness, in addition to the inherent benefits of MEMS technology in terms of linearity and power consumption. A good agreement between measurements and simulations was obtained and highlighted the impact of the fabrication underetching on the device performance. This work constitutes a step forward to the application of such cells in concrete microwave devices such as CRLH-based leaky wave antennas and series feed network and dividers.

Acknowledgment

The authors would like to thank M. Unlu and the METU MEMS Center Staff for their help in the fabrication process development, and F. Bongard for the discussion on the manuscript.

References

[1] G. V. Eleftheriades and K. G. Balmain, *Negative-Refraction Metamaterials: Fundamental Principles and Applications*. Hoboken, NJ: Wiley—IEEE Press, 2005.

[2] C. Caloz and T. Itoh, *Electromagnetic Metamaterials, Transmission Line Theory and Microwave Applications*. Hoboken, NJ: Wiley—IEEE Press, 2006.

[3] J. Perruisseau-Carrier and A. K. Skrivervik, "Composite right/left handed transmission line Metamaterial Phase Shifters (MPS) in MMIC technology," *IEEE Trans. Microw. Theory Tech.*, vol. 54, no. 4, pp. 1582–1589, Apr. 2006.

[4] C. Qin, A. B. Kozyrev, A. Karbassi, and D. W. van der Weide, "Microfabricated V-band left-handed transmission lines," *Metamaterials*, vol. 2, pp. 26–35, Aug. 2007.

[5] C. Damm, J. Freese, M. Schussler, and R. A. Jakoby, "Electrically controllable artificial transmission line transformer for matching purposes," *IEEE Trans. Microw. Theory Tech.*, vol. 55, no. 6, pp. 1348–1354, Jun. 2007.

[6] K. Choul-Young, Y. Jaemo, K. Dong-Wook, and H. Songcheol, "A K-band CMOS voltage controlled delay line based on an artificial left-handed transmission line," *IEEE Microw. Wireless Compon. Lett.*, vol. 18, no. 11, pp. 731–733, Nov. 2008.

[7] M. A. Y. Abdalla, K. Phang, and G. V. Eleftheriades, "Printed and integrated CMOS positive/negative refractive-index phase shifters using tunable active inductors," *IEEE Trans. Microw. Theory Tech.*, vol. 55, no. 8, pp. 1611–1623, Aug. 2007.

[8] J. Perruisseau-Carrier, T. Lisec, and A. K. Skrivervik, "Circuit model and design of silicon-integrated CRLH-TLs analogically controlled by MEMS," *Microw. Optic. Tech. Lett.*, vol. 48, pp. 2496–2499, Dec. 2006.

[9] D. Kuylenstierna, A. Vorobiev, P. Linner, and S. Gevorgian, "Composite right/left handed transmission line phase shifter using ferroelectric varactors," *IEEE Microw. Wireless Compon. Lett.*, vol. 16, no. 4, pp. 167–169, Apr. 2006.

[10] K. Topalli, O. A. Civi, S. Demir, S. Koc, and T. Akin, "A monolithic phased array using 3-bit distributed RF MEMS phase shifters," *IEEE Trans. Microw. Theory Tech.*, vol. 56, no. 2, pp. 270–277, Feb. 2008.

[11] J. Hayden and G. Rebeiz, "Very low-loss distributed X-band and Ka-band MEMS phase shifters using metal-air-metal capacitors," *IEEE Trans. Microw. Theory Tech.*, vol. 51, no. 1, pp. 309–314, Jan. 2003.